JOURNAL OF GUIDANCE, CONTROL, AND DYNAMICS
Vol. 25, No. 1, January–February 2002

Explicit Guidance of Aeroassisted Orbital Transfer Using Matched Asymptotic Expansions

Zeal-Sain Kuo* and Kuo-Chung Liu†
Chung Cheng Institute of Technology, National Defense University, Tao-Yuan 33509, Taiwan, Republic of China

An explicit guidance of aeroassisted orbital transfer by using the method of matched asymptotic expansions is presented. The aeroassisted orbit transfer comprises three consecutive phases: a descending phase entering atmosphere with a negative flight path angle, a transatmospheric flight to deplete its excess energy, and an ascending flight targeting the desired apogee. Feedback control via lift modulation is used to guide the vehicle during the atmospheric fly-through, whereas a matched asymptotic solution for the exit trajectory is available to aim the apogee of the target orbit, thus determining the pull-up condition. The feedback control ensures the stability of a trajectory around the nominal trajectory by compensating for the nonlinear terms in the motion of the vehicle. When the method of matched asymptotic expansions is used, the control algorithms for the explicit guidance are derived and tested against the 1976 U.S. Standard Atmosphere. Simulation results indicate that the control algorithms can effectively control the trajectories in both the lower atmosphere and in the exit phase under the targeting dispersions of atmospheric variations.

Introduction

THE feasibility of constructing advanced space transportation systems has received considerable attention. With the advent of maneuverable aerospace vehicles, the concept of aeroassist for orbital transfer operations has been recognized as one of several critical technologies for future operations. Aeroassisted orbital maneuvering is important in developing space transportation because aeroassisted transfer requires less fuel than the optimal all-propulsive Hohmann transfer for a wide range of high-Earth-orbit (HEO) to low-Earth-orbit (LEO) transfers.[1,2] The research of guidance for aeroassisted orbit transfer (AOT) has also received considerable interest.[3–7] This paper presents an explicit guidance for AOT by using the method of matched asymptotic expansions (MAE).[8,9] The proposed approach employs a feedback control technique to ensure the stability of a trajectory around the nominal trajectory by compensating for the nonlinear terms in the motion of the vehicle. The nominal trajectory generated by MAE is used to develop the control expressions. Because the reference trajectory data are produced analytically, the requirement is decreased for numerical integration or trajectory data storage, thereby reducing the computational burden. The effectiveness of an analytical solution depends on its accuracy. Because of the high accuracy of the solutions obtained by MAE, it is adequate to derive an explicit guidance for transatmospheric motion of AOT.

The analytical solutions derived by this method, called composite solutions, are composed of three parts: outer expansions, inner expansions, and the common limits of both expansions. The composite solutions are constructed by summing up the outer and inner expansions and then subtracting the parts they have in common.[10–13] For atmospheric reentry problems, the outer expansions describe the solutions at a high altitude, nearly in the vacuum, where the gravitational force is predominant, and as such the motion is Keplerian. On the other hand, the inner expansions are the solutions near the planetary surface, where the aerodynamic forces are much stronger than the resultant of gravitational and centrifugal forces. Such solutions are in explicit form, are uniformly valid in both the vacuum and the atmospheric regions, and have been shown to be highly accurate.[8,9] Therefore, it is possible to develop explicit guidance schemes that are robust, of low complexity, and inexpensive.

Complete solutions for AOT by MAE include three arcs: descending arc, ascending arc, and a reference trajectory in the lower layers of atmosphere. The lowest limit of altitude for spacecraft entering into the atmosphere is analytically predicted to provide the starting point of a reference trajectory in the lower atmosphere. Controlling the vehicle in the lower atmosphere is also highly desired because the controllability of aerodynamic forces is nearly singular in the upper atmosphere. Feedback control via lift modulation is then used to guide the spacecraft along the reference trajectory. The analytical predictions provide a reference trajectory as well as determine pull-up conditions. Guidance laws such as constant altitude guidance, constant climb rate, and constant flight-path angle are candidates for flight in the lower atmosphere until a pull-up condition is satisfied. During the ascending phase, the predicted trajectory targeting the apogee is applied to generate an analytic reference trajectory for the exit flight. Control over the ascending phase is again implemented using feedback control via lift modulation along the reference trajectory toward the desired apogee. Once at the apogee, the propulsive system of the vehicle is activated for the final orbit insertion.

HEO-to-LEO Orbital Transfer

The problem of orbital transfer between two coplanar circular orbits was first solved by Hohmann in 1925 (see Ref. 14). It can be shown that for all-propulsive operation the Hohmann transfer is the optimal way to perform this maneuver under the assumption of using a high-thrust propulsive system. In 1961, London demonstrated the possibility of using aerodynamic forces in orbital plane change.[15] For transfer from HEO to LEO in the vicinity of an atmosphere-bearing planet, Mease and Vinh presented a numerical solution for aeroassisted orbital transfer with nearly minimum fuel-consumption.[16] To utilize the analytical MAE solutions, the motion of an AOT vehicle (Fig. 1) starts with a retroburn ΔV_1 at HEO radius r_1 to inject the vehicle into an elliptical transfer orbit with a hypothetical target perigee r_{p1} inside the atmosphere. As it flies through the atmosphere, the vehicle depletes excess kinetic energy. As long as a pull-up condition is satisfied, the vehicle skips out of the atmosphere toward a target apogee with the distance r_2. Then, a second tangential burn ΔV_2 is applied to complete the final insertion into the desired circular LEO. For an idealized aeroassisted transfer, the vehicle grazes the boundary of the atmosphere with radius R.

Presented as Paper 2000-4435 at the AIAA/AAS Astrodynamics Specialist Conference, Denver, CO, 14–17 August 2000; received 6 November 2000; revision received 12 March 2001; accepted for publication 16 March 2001.

*Associate Professor, Department of Mechanical Engineering. Member AIAA.

†Research Assistant, Department of Aeronautical Engineering.

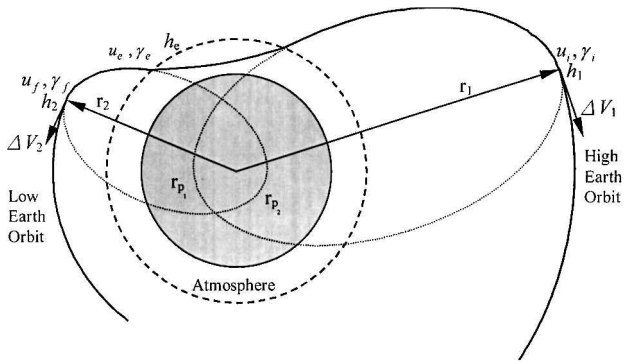

Fig. 1 HEO-to-LEO aeroassisted orbital transfer.

The dimensionless velocity change, normalized with respect to the circular speed $V_c = \sqrt{(gR)}$, is given by

$$\Delta v_A = \Delta V_A / V_c = (\Delta V_1 + \Delta V_2)/V_c = \Delta v_1 + \Delta v_2$$

$$= \left\{ \sqrt{\frac{R}{r_1}} - \sqrt{\frac{2R^2}{r_1(r_1+R)}} + \sqrt{\frac{R}{r_2}} - \sqrt{\frac{2R^2}{r_2(r_2+R)}} \right\} \tag{1}$$

This is the lower bound for any realistic aeroassisted transfer. Compared with the minimum-fuel, all-propulsive transfer mode, the Hohmann transfer, the total dimensionless velocity change is

$$\Delta v_H = \Delta V_H / V_c = \Delta v_1 + \Delta v_2$$

$$= \left\{ \sqrt{\frac{R}{r_1}} - \sqrt{\frac{2r_2R}{r_1(r_1+r_2)}} + \sqrt{\frac{2r_1R}{r_2(r_1+r_2)}} - \sqrt{\frac{R}{r_2}} \right\} \tag{2}$$

As an example, for transfer from GEO ($r_1 = 42241$ km) to a typical space shuttle orbit ($r_2 = 6728$ km), the velocity changes are $\Delta V_H = 3866$ m/s and $\Delta V_A = 1550$ m/s. Notably, the aeroassisted mode results in almost 60% fuel savings over the all-propulsive mode if the heating and aerodynamic penalties are ignored. Unfortunately, the equations of motion for transatmospheric flight generally involve a set of highly nonlinear differential equations, which can only be solved by resorting to numerical integration. Numerical approaches are often confined to a certain set of parameters, for example, the initial conditions, the specific vehicle characteristics, and the atmosphere model. With this in view, several analytical theories have been proposed in the past by various researchers, such as Chapman,[17] Loh,[18] and Yaroshevskii.[19] In these analyses, strong physical assumptions or empirical modifications were made to facilitate the analytical integration. Improved solutions for various reentry problems using the MAE method have been developed.[8,9] The MAE method is a powerful tool in the analysis of AOT vehicle motion because it incorporates the knowledge of the physical characteristics at the two-end boundaries of the reentry problem and rigorous mathematical procedures. In our previous work using MAE, we obtained accurate and explicit analytical solutions that were uniformly valid from the vacuum through the atmosphere for a variety of flight conditions. We now proceed to consider the guidance and control problem of AOT vehicles under the influence of aerodynamic and atmospheric uncertainties by utilizing the matched asymptotic solutions.

Governing Equations

Consider a general case of planar atmospheric flight of an AOT vehicle, moving about a spherical planet with a nonrotating atmosphere. When Fig. 2 is referred to and standard notation is used, the governing equations are given by

$$\frac{dr}{dt} = V \sin\gamma, \qquad \frac{d\theta}{dt} = \frac{V\cos\gamma}{r}$$

$$\frac{dV}{dt} = -\frac{\rho A C_D V^2}{2m} - g\sin\gamma$$

$$V\frac{d\gamma}{dt} = \frac{\rho A C_L V^2}{2m} - \left(g - \frac{V^2}{r}\right)\cos\gamma \tag{3}$$

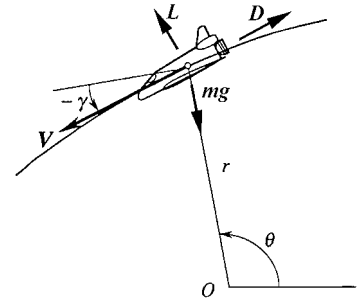

Fig. 2 Trajectory variables.

It is assumed that when $r > R$ the flight is Keplerian. Hence, we shall assume that the central gravitational field obeys the Newtonian inverse square law, that is,

$$g = g_s\left(r_s^2/r^2\right) \tag{4}$$

where subscript s denotes values at sea level. Furthermore, the lift and drag coefficients are normalized by C_L^* and C_D^*, respectively,

$$C_L = \lambda C_L^*, \qquad C_D = C_D^*(1+\lambda^2)/2 \tag{5}$$

where λ is the normalized lift control and superscript * denotes the coefficients corresponding to the maximum lift-to-drag ratio E^*. Moreover, we have assumed that the drag polar is parabolic. When the following dimensionless variables and parameters are used,

$$u = V^2/g_s r_s, \qquad h = (r - r_s)/r_s, \qquad B = \rho_s A C_L^*/2m\beta,$$

$$\rho = \rho_s \exp(-h/\varepsilon), \qquad \varepsilon = 1/\beta r_s \tag{6}$$

the dimensionless equations of motion can be written as

$$\frac{d\theta}{dh} = \frac{1}{(1+h)\tan\gamma}$$

$$\frac{du}{dh} = -\frac{2}{(1+h)^2} - \frac{B(1+\lambda^2)\,u\exp(-h/\varepsilon)}{\varepsilon E^*\sin\gamma}$$

$$\frac{d\gamma}{dh} = \left\{\frac{1}{(1+h)} - \frac{1}{u(1+h)^2}\right\}\frac{1}{\tan\gamma} + \frac{B\lambda\,\exp(-h/\varepsilon)}{\varepsilon\sin\gamma} \tag{7}$$

where ε is a small parameter because βr_s is large. For the Earth's atmosphere, approximately $\beta r_s = 900$. Equations (7) constitute the most appropriate dimensionless equations of motion for developing the guidance and control of AOT vehicles using the MAE method with lift modulation. Note that the θ equation is not involved in the following analysis because θ is an ignorable coordinate for circular-to-circular orbital transfer.

Solutions by MAE

The analytical solutions for AOT by MAE include three arcs: descending arc, ascending arc, and a reference trajectory in the lower layers of atmosphere. Solutions derived by this method, called composite solutions, are composed of three parts: outer expansions, inner expansions, and the common limits of both expansions. The composite solutions are formulated by adding the outer and inner expansions and then subtracting the common limits under an appropriate matching principle. Based on the zero-order composite solutions, the first-order solutions are obtained by generating perturbation equations for the small discrepancies between the zero-order composite solutions and the exact equations. Then, the perturbation equations are integrated separately near the boundaries to obtain the perturbed outer and inner expansions for a first-order matching.

Outer Expansions (Keplerian Region)

The outer expansions describe the solutions at a high altitude, nearly in the vacuum where $\exp(-h/\varepsilon) \to 0$. Here the gravitational

force is predominant. Assume the following expansions with the state vector $\boldsymbol{x} = [u, \gamma]^T$

$$\boldsymbol{x} = \boldsymbol{x}_0(h) + \varepsilon \boldsymbol{x}_1(h) + \varepsilon^2 \boldsymbol{x}_2(h) + \cdots \tag{8}$$

By substitution into Eq. (7) and when the outer limit is taken as $\varepsilon \to 0$ with the altitude variable and other dimensionless variables held fixed, the zero-order equations in the outer expansions are

$$\frac{\mathrm{d}u_0}{\mathrm{d}h} = -\frac{2}{(1+h)^2}$$

$$\frac{\mathrm{d}\gamma_0}{\mathrm{d}h} = \left\{\frac{1}{(1+h)} - \frac{1}{u_0(1+h)^2}\right\}\frac{1}{\tan\gamma_0} \tag{9}$$

Note that the effect of making $\varepsilon \to 0$ is equivalent to taking the atmosphere to the region near the vacuum. These are the equations for Keplerian motion. The outer solutions are

$$u_0 = u_i + 2\left(\frac{1}{(1+h)} - \frac{1}{(1+h_1)}\right), \qquad \cos\gamma_0 = \frac{(1+h_1)\sqrt{u_i}}{(1+h)\sqrt{u_0}} \tag{10}$$

where u_i is the initial speed of the elliptical transfer orbit at apogee h_1. At atmospheric entry, we can obtain the entry conditions by evaluating Eq. (10) at the entry altitude h_e.

Inner Expansions (Aerodynamic Predominant Region)

Using a stretching transformation

$$\bar{h} = h/\varepsilon \tag{11}$$

the inner expansions are introduced to study the rapid change of motion near the surface of the planet where the aerodynamic force is dominant. We assume the following expansions:

$$\boldsymbol{x} = \bar{\boldsymbol{x}}_0(\bar{h}) + \varepsilon \bar{\boldsymbol{x}}_1(\bar{h}) + \varepsilon^2 \bar{\boldsymbol{x}}_2(\bar{h}) + \cdots \tag{12}$$

By substitution into the Eq. (7) and when the inner limit is taken as $\varepsilon \to 0$ with the new altitude variable $\bar{h}$ and other dimensionless variables held fixed, the zero-order equations for the inner expansions are

$$\frac{\mathrm{d}\bar{u}_0}{\mathrm{d}\bar{h}} = -\frac{B(1+\lambda^2)\bar{u}_0 e^{-\bar{h}}}{E^* \sin\bar{\gamma}_0}, \qquad \frac{\mathrm{d}\bar{\gamma}_0}{\mathrm{d}\bar{h}} = \frac{B\lambda e^{-\bar{h}}}{\sin\bar{\gamma}_0} \tag{13}$$

The zero-order equations can also be easily integrated to yield the inner solutions

$$\bar{u}_0 = \bar{C}_1 \exp\left[-\frac{(1+\lambda^2)}{\lambda E^*}\bar{\gamma}_0\right]$$

$$\cos\bar{\gamma}_0 = B\lambda \exp(-h/\varepsilon) + \bar{C}_2 \tag{14}$$

where $\bar{C}_1$ and $\bar{C}_2$ are the corresponding constants of integration to be determined by matching with the outer expansions.

Zero-Order Composite Solutions

The zero-order composite solutions are constructed by summing up the outer and inner solutions and subtracting the parts they have in common to obtain the matched asymptotic solutions uniformly valid over both the outer and the inner regions, that is,

$$\boldsymbol{x}_c = \boldsymbol{x}_0 + \bar{\boldsymbol{x}}_0 - \boldsymbol{x}_\infty \tag{15}$$

where $\boldsymbol{x}_\infty$ is the common limit defined by the matching principle

$$\boldsymbol{x}_\infty = \lim_{h \to h_b} \boldsymbol{x}_0(h) = \lim_{h \to \infty} \bar{\boldsymbol{x}}_0(\bar{h}) \tag{16}$$

We easily obtain the zero-order composite solutions

$$u_c = 2\left(\frac{1}{1+h} - \frac{1}{1+h_b}\right) + \bar{C}_1 \exp\left[-\frac{(1+\lambda^2)}{\lambda E^*}\bar{\gamma}_0\right]$$

$$\cos\gamma_c = \frac{(1+h_1)\sqrt{u_i}}{(1+h)\sqrt{u_0}} + B\lambda \exp(-h/\varepsilon) \tag{17}$$

By using the matching condition (16), we have the relations between $\bar{C}_1$ and $\bar{C}_2$ and the outer expansions:

$$u_i + 2\left(\frac{1}{1+h_b} - \frac{1}{1+h_1}\right) = \bar{C}_1 \exp\left[-\frac{(1+\lambda^2)}{\lambda E^*}\cos^{-1}(\bar{C}_2)\right]$$

$$\frac{(1+h_1)\sqrt{u_i}}{(1+h_b)\sqrt{u_0(h_b)}} = \bar{C}_2 \tag{18}$$

where h_b is defined as the lowest limit of altitude for entry trajectory with $\gamma_c(h_b) = 0$, that is,

$$1 = B\lambda \exp(-h_b/\varepsilon) + \bar{C}_2 \tag{19}$$

First-Order Solutions

The first-order solutions are obtained by considering the small discrepancies between the exact equations and the zero-order composite solutions. We first construct the perturbation equations by letting

$$u = u_c + z = u_0 + \bar{u}_0 - u_\infty + z$$

$$\cos\gamma = \cos\gamma_c + q = \cos\gamma_0 + \cos\bar{\gamma}_0 - \cos\gamma_\infty + q \tag{20}$$

Substituting into the dimensionless governing equations (7) and using the equations of outer and inner expansions for simplification, we obtain the equations for the small perturbations z and q:

$$\frac{\mathrm{d}z}{\mathrm{d}h} = -\frac{B(1+\lambda^2)u\exp(-h/\varepsilon)}{\varepsilon E^* \sin\gamma} + \frac{B(1+\lambda^2)\bar{u}_0 \exp(-h/\varepsilon)}{\varepsilon E^* \sin\bar{\gamma}_0}$$

$$\frac{\mathrm{d}q}{\mathrm{d}h} = -\left\{\frac{1}{(1+h)} - \frac{1}{u(1+h)^2}\right\}\cos\gamma + \left\{\frac{1}{(1+h)} - \frac{1}{u_0(1+h)^2}\right\}\cos\gamma_0 \tag{21}$$

The initial conditions for z and q are

$$z(h_e) = 0, \qquad q(h_e) = 0 \tag{22}$$

where h_e denotes the entry altitude. Again we integrate the equations for the perturbations separately first in the outer region and then in the inner region. On integrating in the outer region, we have the outer solutions for the perturbation z and q

$$z_0 = C_3 = 0, \qquad q_0 = C_4 \Big/ \sqrt{C_1(1+h)^2 + 2(1+h)} \tag{23}$$

where C_3 and C_4 are the constants of integration.

In the inner region, the inner expansions are obtained by repeated application of the inner limit with the inner variable $\bar{h} = h/\varepsilon$ and other dimensionless variables held fixed. The analytical derivation is long and tedious and so we summarize it as follows: First, we anticipate the inner expansions for the perturbations in the form

$$z^i = \bar{z}_0(\bar{h}) + \varepsilon \bar{z}_1(\bar{h}) + \varepsilon^2 \bar{z}_2(\bar{h}) + \cdots$$

$$q^i = \varepsilon\left[\bar{q}_0(\bar{h}) + \varepsilon \bar{q}_1(\bar{h}) + \varepsilon^2 \bar{q}_2(\bar{h}) + \cdots\right] \tag{24}$$

Then, substituting into Eq. (21) and separating terms of different order in ε, we integrate the zero-order equations of the perturbations

in the inner region. It is pointed out that inner expansions for $\bar{z}_0$ are not integrable,[8] but $\bar{q}_0$ can be integrated nearly exactly with the following limiting and approximate conditions:

$$u \to \bar{u}_0 + z \approx \bar{u}_0, \qquad z \ll 1$$

$$\cos\gamma \to \cos\bar{\gamma}_0 + q \approx \cos\bar{\gamma}_0, \qquad q \ll 1 \tag{25}$$

On integrating, we have the inner solution for $\bar{q}_0$

$$\bar{q}_0 = \frac{B\lambda e^{-\bar{h}}}{(1+h_b)} - \frac{\bar{C}_2}{\varepsilon}\ell_n(1+\varepsilon\bar{h}) + \frac{k\sin\bar{\gamma}_0 - \cos\bar{\gamma}_0}{\bar{u}_0(1+h_b)^2(1+k^2)} + \frac{\bar{C}_2}{\bar{C}_1(1+h_b)^2}\left[\bar{h} + kF_1(\bar{h}) + \frac{k^2}{2!}F_2(\bar{h}) + \frac{k+k^3}{3!}F_3(\bar{h}) + \cdots\right] - \frac{1}{\varepsilon}\cos\gamma_0 + \bar{C}_4 \tag{26}$$

where we have defined

$$k = \frac{(1+\lambda^2)}{\lambda E^*}$$

$$F_1(\bar{h}) = \sqrt{\mu}\ell_n\left[2\frac{\mp\sqrt{\mu}\sin\bar{\gamma}_0 - \bar{C}_2\cos\bar{\gamma}_0 + 1}{\cos\bar{\gamma}_0 - \bar{C}_2}\right] - [\mp\sin\bar{\gamma}_0 \mp \bar{C}_2\bar{\gamma}_0]$$

$$F_2(\bar{h}) = \mu\bar{h} + \tfrac{1}{2}(\cos\bar{\gamma}_0 - \bar{C}_2)(\cos\bar{\gamma}_0 + 3\bar{C}_2)$$

$$F_3(\bar{h}) = \mu F_1(\bar{h}) \mp \left[\tfrac{1}{2}\bar{C}_2\bar{\gamma}_0 - (\bar{C}_2/4)\sin 2\bar{\gamma}_0 + \tfrac{1}{3}\sin^3\bar{\gamma}_0\right]$$

$$\cdots \tag{27}$$

and

$$\mu = 1 - \bar{C}_2^2 \tag{28}$$

We take the minus sign for descending arc and the plus sign for ascending arc in Eq. (27). The composite solution $q_c(h)$ is constructed by combining the outer and inner solutions and relating the integration constants by asymptotic matching with the initial conditions Eq. (22). Then, according to Eq. (20), the first-order composite solution for γ is

$$\cos\gamma_c' = \frac{(1+h_1)\sqrt{u_i}}{(1+h)\sqrt{u_0}} + B\lambda\exp(-h/\varepsilon) + \bar{C}_2' - \frac{(1+h_1)\sqrt{u_i}}{(1+h_b')\sqrt{u_0(h_b')}} + \varepsilon q_c(h) \tag{29}$$

The first-order solution and the corresponding integration constants are now accented with a prime because we need to reevaluate all of the constants of integration and the condition for the lowest altitude is now $\cos\gamma_c' = 1$, that is,

$$B\lambda\exp(-h_b'/\varepsilon) + \bar{C}_2' + \varepsilon q_c(h_b') = 1 \tag{30}$$

The solution for speed is also improved because we have new values for the constants of integration and the lowest altitude h_b',

$$u_c' = 2\left(\frac{1}{1+h} - \frac{1}{1+h_b'}\right) + \bar{C}_1'\exp\left[-\frac{(1+\lambda^2)}{\lambda E^*}\bar{\gamma}_0'\right] \tag{31}$$

Explicit Guidance for Lift Modulation

The transatmospheric motion in the AOT is considered in this section. Because the analytic solutions obtained by MAE have been shown to be very accurate,[8,9] it is desired to generate autonomous guidance and control strategies under the consideration of parameter uncertainties and unknown disturbances such as system modeling uncertainty, atmospheric density fluctuation, aerodynamic coefficient dispersion, and navigation errors.

Trajectory Tracking

Using dimensionless variables and the assumptions described in Eqs. (4–6), the equations of motion are written as follows:

$$\frac{\mathrm{d}h}{\mathrm{d}\bar{t}} = \sqrt{u}\sin\gamma, \qquad \frac{\mathrm{d}\theta}{\mathrm{d}\bar{t}} = \frac{\sqrt{u}}{(1+h)}\cos\gamma$$

$$\frac{\mathrm{d}u}{\mathrm{d}\bar{t}} = -\frac{B(1+\lambda^2)u^{\frac{3}{2}}\exp(-h/\varepsilon)}{\varepsilon E^*} - \frac{2\sqrt{u}}{(1+h)^2}\sin\gamma$$

$$\frac{\mathrm{d}\gamma}{\mathrm{d}\bar{t}} = \frac{B\lambda\sqrt{u}\exp(-h/\varepsilon)}{\varepsilon} + \left[\frac{\sqrt{u}}{(1+h)} - \frac{1}{\sqrt{u}(1+h)^2}\right]\cos\gamma \tag{32}$$

where we have defined the dimensionless time as $\bar{t} \equiv V_s t/r_s$, and $V_s = \sqrt{(g_s r_s)}$ is the circular speed at the reference altitude. Equation (32) renders a suitable form to develop guidance and control algorithms using MAE solutions. The control for trajectory tracking is derived through an equilibrium glide algorithm following a reference trajectory. The control for equilibrium glide is based on the radial component of the equation of motion. From Fig. 2 and Eq. (3), the radial component of the equation of motion is

$$m\frac{\mathrm{d}^2 r}{\mathrm{d}t^2} = L_r - D_r + m\frac{(V\cos\gamma)^2}{r} - mg \tag{33}$$

where L_r and D_r are the radial components of the lift and drag, respectively. By using dimensionless variables u and h to replace V and r, we have

$$\frac{\mathrm{d}^2 h}{\mathrm{d}\bar{t}^2} = \frac{Bu\exp(-h/\varepsilon)}{2\varepsilon E^*}[2\lambda E^*\cos\gamma - (1+\lambda^2)\sin\gamma] + \frac{u\cos^2\gamma}{(1+h)} - \frac{1}{(1+h)^2} \tag{34}$$

This equation can also be derived from Eq. (32) by applying the chain rule of calculus. Define a pseudocontrol as the ratio of the acceleration to the gravity acceleration

$$\eta \equiv (L_r - D_r)/mg_s = \frac{\rho A V^2}{2mg_s}(C_L\cos\gamma - C_D\sin\gamma) \tag{35}$$

For equilibrium altitude change rate, we set Eq. (33) to be zero, which yields

$$\eta = \frac{1}{(1+h)^2} - \frac{u\cos^2\gamma}{(1+h)} \tag{36}$$

This value of control yields an equilibrium altitude change rate. To establish equilibrium altitude rate for asymptotic tracking, an altitude damper is required. The control equation for the commanded pseudocontrol is defined as

$$\eta_c = \frac{1}{(1+h)^2} - \frac{u\cos^2\gamma}{(1+h)} - K_{\dot{h}}(\dot{h} - \dot{h}_{\mathrm{ref}}) \tag{37}$$

where $K_{\dot{h}}$ is the feedback gain for altitude rate and $\dot{h}_{\mathrm{ref}}$ is the reference altitude rate obtained by using MAE solutions, that is,

$$\dot{h}_{\mathrm{ref}} = \sqrt{u_c}\sin\gamma_c \tag{38}$$

This indicates that the reference altitude change rate is an explicit function of the altitude. When Eqs. (35) and (37) are substituted into Eq. (33), the radial equation of motion becomes

$$\ddot{h} + K_{\dot{h}}\dot{h} = K_{\dot{h}}\dot{h}_{\mathrm{ref}} \tag{39}$$

Equation (39) results in a linear first-order differential equation for the altitude rate tracking with a time constant chosen to achieve the desired vehicle response:

$$\tau = 1/K_{\dot{h}} \tag{40}$$

On using dimensionless variables, the pseudocontrol in Eq. (35) is written as

$$\eta_c = \frac{Bu\exp(-h/\varepsilon)}{2\varepsilon E^*}\left[2\lambda_c E^*\cos\gamma - \left(1+\lambda_c^2\right)\sin\gamma\right] \tag{41}$$

This is the radial force required per unit mass for equilibrium altitude rate. Notably, the $\sin\gamma$ term in Eq. (41) can be neglected because the flight-path angle stays small within a few degrees and the nominal value for λ_c is near maximum to recover from the downward plunge with large C_L and, correspondingly, at a higher C_D. Then, the approximate actual lift control for trajectory tracking is solved in terms of the pseudo-control:

$$\lambda_c \approx \frac{\varepsilon\sec\gamma}{Bu\exp(-h/\varepsilon)}\eta_c \tag{42}$$

This guidance is explicit because it is expressed in terms of current state instead of the derivative of the current state with respect to a nominal state. Note that the approximation used for the control law is not necessary, but it has the advantage of revealing explicitly the various effects of the speed, flight-path angle, local density, and the parameter B. Nevertheless, the exact relation for the control law will also be given later.

Guidance at Lower Layers of Atmosphere

As the vehicle enters the atmosphere, analytical prediction of the lowest altitude using MAE solutions is provided to be the starting point of a reference trajectory in the lower layers of atmosphere. Guidance laws such as constant altitude guidance, constant climb rate, and constant flight-path angle are candidates for flight in the lower atmosphere until a pull-up condition is satisfied. In this paper, the control for constant altitude guidance is considered because the vehicle is not responsive to the aerodynamic forces in the higher layers of atmosphere due to rare density. The pseudocontrol to track a reference altitude is defined as

$$\eta_c = \frac{1}{(1+h)^2} - \frac{u\cos^2\gamma}{(1+h)} - K_{\dot h}(\dot h - \dot h_{\text{ref}}) - K_h(h - h_{\text{ref}}) \tag{43}$$

Again, $\dot h$ is the altitude change rate and $K_{\dot h}$ and K_h are the feedback gains for the altitude rate and altitude, respectively. For guidance at the lowest altitude h_b, we have

$$\dot h_{\text{ref}} = 0, \qquad h_{\text{ref}} = h_b \tag{44}$$

Then the radial equation of motion becomes

$$\ddot h + K_{\dot h}\dot h + K_h h = K_h h_b \tag{45}$$

This is a linear first-order differential equation for the altitude with the following natural frequency and damping ratio:

$$\omega_n = \sqrt{K_h}, \qquad \zeta = K_{\dot h}/2\omega_n \tag{46}$$

The control is nearly exact because for constant altitude flight the flight-path angle is extremely close to zero:

$$\lambda_c = \frac{\varepsilon\sec\gamma}{Bu\exp(-h/\varepsilon)}\eta_c = \frac{\varepsilon\eta_c}{Bu\exp(-h/\varepsilon)} \tag{47}$$

Pull-Up Condition and Apogee Targeting

During the atmospheric fly-through, the vehicle depletes its excess kinetic energy, whereas an analytical prediction by using the MAE solutions provides a reference exit trajectory targeting the desired apogee, thus determining the pull-up condition. The pull-up condition has the form

$$u = u_p = \text{free}, \qquad \gamma = \gamma_p = \text{given}, \qquad \text{at} \qquad h = h_p \tag{48}$$

where the pull-up speed is to be determined by matching from outer to inner solutions. The conditions at exit and at apogee are given as follows:

$$u_e = \text{free}, \qquad \gamma_e = \text{free}, \qquad \text{at} \qquad h = h_e \tag{49}$$

$$u_f = \text{free}, \qquad \gamma_f = 0, \qquad \text{at} \qquad h = h_2 \tag{50}$$

Here u_f is free, but it is desired to reach the apogee with as much velocity as possible to minimize the ΔV for the final insertion. However, the state variables (u, γ) are coupled. Variables u and γ are not determined individually when we apply the MAE solutions. Therefore, using Eqs. (10), (14–17), and the composite solution $q_c(h)$, we reevaluate all constants of integration and construct the composite solutions for the ascending trajectory,

$$u_c = 2\left(\frac{1}{1+h} - \frac{1}{1+h_b}\right) + \bar C_{1e}\exp\left[+\frac{(1+\lambda^2)}{\lambda E^*}\bar\gamma_0\right]$$

$$\cos\gamma_c = \frac{(1+h_2)\sqrt{u_f}}{(1+h)\sqrt{u_0}} + B\lambda\exp(-h/\varepsilon)$$

$$+\bar C_{2e} - \frac{(1+h_2)\sqrt{u_f}}{(1+h_b)\sqrt{u_0(h_b)}} + \varepsilon q_c(h) \tag{51}$$

The matching condition is

$$u_f + 2\left(\frac{1}{1+h_b} - \frac{1}{1+h_2}\right) = \bar C_{1e}\exp\left[+\frac{(1+\lambda^2)}{\lambda E^*}\cos^{-1}(\bar C_{2e})\right]$$

$$\frac{(1+h_2)\sqrt{u_f}}{(1+h_b)\sqrt{u_0(h_b)}} = \bar C_{2e} \tag{52}$$

where subscript $1e$ and $2e$ denote the constants of integration for exit trajectory and the accented prime is removed for simplicity. With $\gamma = 0$ and γ_p given at $h = h_p$, we actually have four unknowns, namely, C_{1e}, C_{2e}, u_p, and u_f, to be evaluated from Eqs. (51) and (52). Now, the exit condition is no longer free and can be solved uniquely by evaluating Eq. (51) at $h = h_e$:

$$u_c(h_e) = 2\left(\frac{1}{1+h_e} - \frac{1}{1+h_b}\right) + \bar C_{1e}\exp\left[\frac{(1+\lambda^2)}{\lambda E^*}\bar\gamma_0(h_e)\right]$$

$$\cos\gamma_c(h_e) = \frac{(1+h_2)\sqrt{u_f}}{(1+h_e)\sqrt{u_0(h_e)}} + B\lambda\exp(-h_e/\varepsilon) + \varepsilon q_c(h_e) \tag{53}$$

For the case of constant altitude guidance at the lowest altitude, we have the pull-up condition

$$u_p = \bar C_{1e}, \qquad \gamma_p = 0, \qquad \text{at} \qquad h = h_p = h_b \tag{54}$$

since

$$u_p = 2\left(\frac{1}{1+h_p} - \frac{1}{1+h_b}\right) + \bar C_{1e}\exp\left[\frac{(1+\lambda^2)}{\lambda E^*}\bar\gamma_0(h_b)\right] = \bar C_{1e} \tag{55}$$

Note that the pull-up speed is merely the inner constant of integration for the speed. Because the pull-up condition is determined, the exit condition and the speed at apogee for the case of constant altitude guidance can be solved uniquely by using MAE solutions. The speed at the apogee will be

$$u_f = 2\left(\frac{1}{1+h_2} - \frac{1}{1+h_b}\right) + \bar C_{1e}\exp\left[\frac{(1+\lambda^2)}{\lambda E^*}\cos^{-1}(\bar C_{2e})\right] \tag{56}$$

To target the prescribed apogee altitude h_2 after exit from the atmosphere, the exit condition must satisfy the following constraint, which is derived from conservation of energy and the conservation of angular momentum along the ascending trajectory to the apogee:

$$u_e\left[(1+h_2)^2 - (1+h_e)^2\cos^2\gamma_e\right] = 2(1+h_2)(h_2 - h_e)/(1+h_e) \tag{57}$$

Using running state variables (u, γ) at h to replace the exit condition and solving for h_2, we are able to compute the resultant apogee continuously along the ascending trajectory:

$$h_2 = \alpha\left[1 \pm \sqrt{1 - (2 - \alpha u)\alpha u \cos^2\gamma}\right]\Big/(2 - \alpha u) - 1 \qquad (58)$$

where we have defined $\alpha = 1 + h$ and the minus sign is for the hypothetical perigee r_{p2} inside the atmosphere.

Exact Control Law

The actual control law λ_c can be solved exactly in terms of the current state and the pseudocontrol η_c. From Eq. (41), define κ_c as

$$\kappa_c = 2\lambda_c E^* \cos\gamma - \left(1 + \lambda_c^2\right)\sin\gamma \qquad (59)$$

Then, Eq. (41) becomes

$$\eta_c = \kappa_c \frac{Bu\exp(-h/\varepsilon)}{2\varepsilon E^*} \qquad (60)$$

Because the $\sin\gamma$ term is no longer neglected, Eq. (59) is rearranged into a quadratic equation of λ_c,

$$\lambda_c^2 \sin\gamma - 2\lambda_c E^* \cos\gamma + \kappa_c + \sin\gamma = 0 \qquad (61)$$

Solving the quadratic equation yields the exact control law

$$\lambda_c = E^* \cot\gamma \pm \sqrt{E^{*2}\cot^2\gamma - (1 + \kappa_c \csc\gamma)} \qquad (62)$$

where the plus sign is for negative flight-path angle, minus is for positive flight-path angle, and κ_c is a function of speed, altitude, and the pseudocontrol,

$$\kappa_c = \frac{2\varepsilon E^*}{Bu\exp(-h/\varepsilon)}\eta_c \qquad (63)$$

However, it is seen that, in the exact control law Eq. (62), trigonometric functions, cotangent and cosecant, are involved. Thus, the control is sensitive to truncation error in computation for flight with small angle due to singularity at $\gamma = 0$. To overcome this weakness, a better approach for the exact control is presented here for comparison. First, we define a mathematical parameter γ_E as

$$\tan\gamma_E = \frac{2\lambda_c E^*}{\left(1 + \lambda_c^2\right)} \qquad (64)$$

and, conversely,

$$\lambda_c = E^*/\tan\gamma_E \pm \sqrt{(E^*/\tan\gamma_E)^2 - 1} \qquad (65)$$

Then, substituting into Eq. (59) and using addition and product formulas of trigonometric functions yields

$$\kappa_c = \sqrt{4\lambda_c^2 E^{*2} + \left(1 + \lambda_c^2\right)^2}\,\sin(\gamma_E - \gamma) \qquad (66)$$

Solving for γ_E, we have

$$\gamma_E = \gamma + \sin^{-1}\left[\kappa_c \Big/ \sqrt{4\lambda_c^2 E^{*2} + \left(1 + \lambda_c^2\right)^2}\right] \qquad (67)$$

Using Eq. (65), we have a nonlinear equation for γ_E:

$$\kappa_c = \frac{2\sin(\gamma_E - \gamma)}{\cos\gamma_E}\left(\frac{E^*}{\tan\gamma_E}\right)\left[\frac{E^*}{\tan\gamma_E} \pm \sqrt{\left(\frac{E^*}{\tan\gamma_E}\right)^2 - 1}\right] \qquad (68)$$

For given speed and altitude, that is, given κ_c, and the flight-path angle γ, we first compute γ_E, and then deduce the exact control law using Eq. (65).

The exact control law is advantageous in the sense that it reveals the relation of the control law with respect to the ratio of maximum lift-to-drag ratio to the lift-to-drag ratio required, that is, $E^*/\tan\gamma_E = E^*/E$. Furthermore, for flight at the maximum lift-to-drag ratio, $E = E^*$, Eq. (65) gives $\lambda_c = 1$.

Numerical Example

This study develops an explicit guidance and obtains feedback controls for AOT against parameter uncertainties and unknown disturbances such as system modeling errors, atmospheric density fluctuation, aerodynamic coefficient dispersion, and navigation errors. As a numerical example, the case of transfer from geostationary Earth orbit (GEO) ($r_1 = 42241$ km) to 350 km altitude LEO ($r_2 = 6728$ km) with constant altitude guidance in the lower layers of atmosphere is considered. The exponential density model and the 1976 U.S. Standard Atmosphere[20] (US-76) are also considered for comparison. The transfer initiates with an in-plane tangential retroburn deorbit. The vehicle is then injected into an elliptical transfer orbit with a hypothetical target perigee r_{p1} inside the atmosphere. The vehicle has a maximum lift-to-drag ratio of $E^* = 1$, and the physical parameter selected for the vehicle is $B = 2.68$. This would provide a sensible aerodynamic force to start the entry at an altitude of 120 km. To generate the reference trajectories, the nominal value of the lift control λ is unity for entry and exit maneuvers, which corresponds to flying at the maximum lift-to-drag ratio. Figures 3

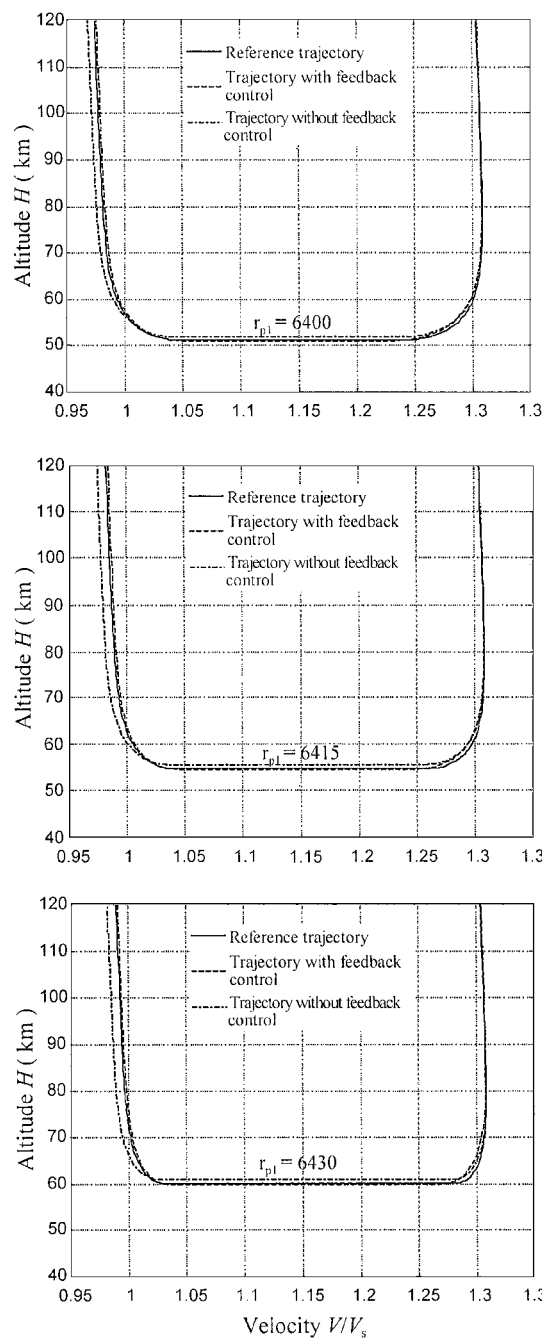

Fig. 3 Variations of velocity as functions of the altitude for various hypothetical target perigees.

and 4 plot the variations of the velocity and the flight-path angle as functions of the altitude for various r_{p1}, 6400, 6415, 6430 km, respectively. For the flight at the lowest altitude, the constant altitude guidance is applied to all cases with $K_h = 0.42$ and $K_h = 0.09$. In Figs. 3 and 4, the solid lines denote the reference trajectories generated by MAE method. The dashed lines represent the trajectories computed by numerical integration with feedback control under the influence of US-76 atmospheric density dispersion, whereas the dashed–dotted lines refer to the trajectories without feedback control. The feedback gain of altitude rate damper $K_h = 0.2$, or equivalently $\tau = 5$ s, for trajectory tracking during entry and exit phases. Figures 3 and 4 show that the errors of the dashed–dotted lines propagate along the trajectories. On the other hand, a high degree

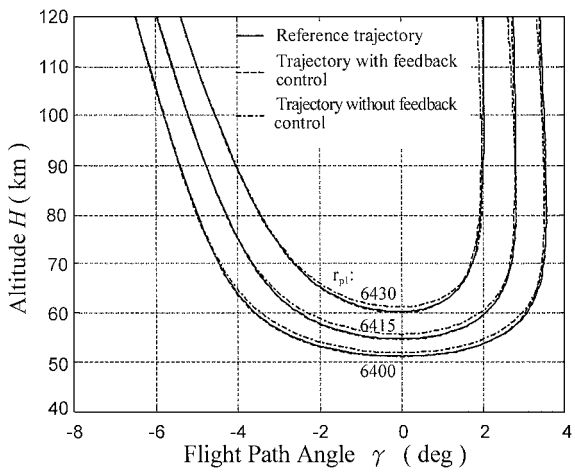

Fig. 4 Variations of flight-path angle as functions of the altitude for various hypothetical target perigees.

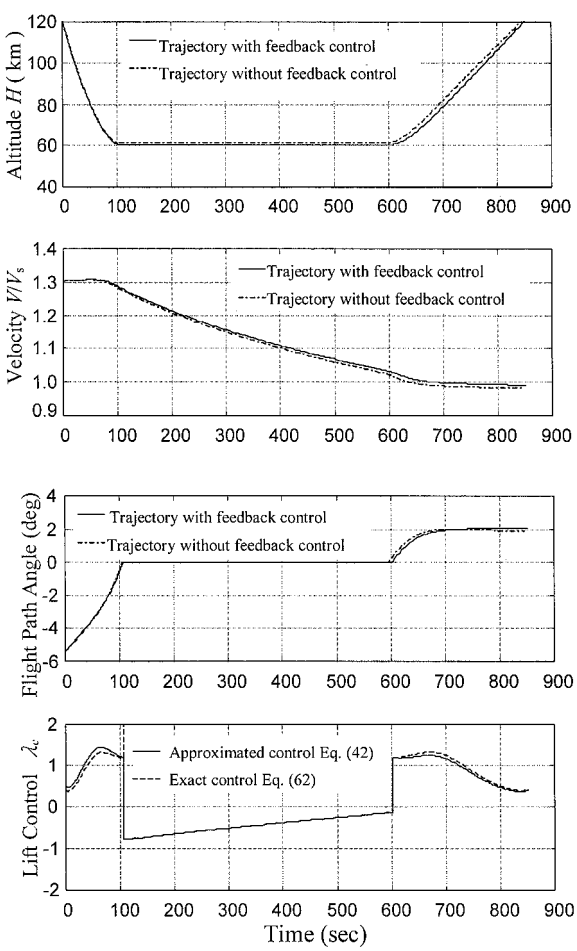

Fig. 5 Time history of state variables and the lift control.

Table 1 Trajectory elements and characteristic velocity changes

	r_{p1} km		
Parameter	6400	6415	6430
V_i, m/s	10315.86	10316.10	10316.35
γ_i, deg	−6.4939	−5.9733	−5.4039
ΔV_1, m/s	1496.91	1495.31	1493.70
H_b, km			
Reference trajectory	51.15028	54.67923	60.14582
US-76	51.87430	55.59558	61.04770
Traj W/FB	51.03356	54.53527	59.96581
V_p, m/s			
Reference trajectory	8296.01	8241.43	8160.75
US-76	8245.55	8180.52	8107.95
Traj W/FB	8314.99	8261.20	8182.10
V_e, m/s			
Reference trajectory	7716.45	7780.19	7835.78
US-76	7661.68	7709.71	7766.72
Traj W/FB	7741.11	7804.48	7861.18
γ_e, deg			
Reference trajectory	3.415812	2.764273	2.040321
US-76	3.325152	2.624797	1.875570
Traj W/FB	3.378347	2.727480	2.006007
ΔV_2, m/s			
Reference trajectory	262.02	196.27	138.37
US-76	286.91	219.75	145.88
Traj W/FB	248.95	187.83	137.74
$\Delta V_1 + \Delta V_2$			
Reference trajectory	1758.93	1691.58	1632.07
US-76	1783.82	1715.06	1639.58
Traj W/FB	1745.86	1683.14	1631.44
Fuel saving, %			
Reference trajectory	54.5	56.3	57.8
US-76	53.9	55.6	57.6
Traj W/FB	54.8	56.5	57.8
r_2, km			
Reference trajectory	6727.83	6728.00	6728.06
US-76	6676.58	6647.80	6622.31
Traj W/FB	6748.42	6756.44	6771.60

of accuracy is achieved during the constant altitude flight and the exit phase with feedback controls.

Figure 5 shows the time histories of the state variables and the lift controls for the case of $r_{p1} = 6430$ km. Notably, the dashed line in the subplot of lift control is computed by using the exact control law Eq. (62) for comparison with the approximate control law Eq. (42). The subplot of lift control indicates that, at about time = 110 s, the control computed by the exact control law (dashed line) becomes infinity due to the singularity at $\gamma = 0$. Table 1 summarizes the numerical results of the trajectory elements and the characteristic velocity changes for the orbital transfer with and without feedback control. According to Table 1, the error at the lowest altitude for the worst case ($r_{p1} = 6430$ km) is merely 180 m, corresponding to a relative error of 0.3%, for the trajectory with feedback control (Traj W/FB), whereas it has an error of 902 m for the trajectory without feedback (US-76). Note that the trajectories for the cases with and without feedback both operate under the fluctuation of US-76 atmospheric density. Errors for the pull-up velocity range from 19 to 21 m/s and 50 to 61 m/s for the cases with and without feedback, respectively. As expected, the orbit targeting error markedly decreases when using the explicit guidance based on the MAE solutions under the influence of atmospheric density variations.

Table 1 also lists the characteristic velocity changes for all cases. The values for ΔV_1 are very close, that is, only a difference of 3.21 m/s at most, because it is insensitive with respect to r_{p1}, as pointed out in Ref. 10. On the other hand, ΔV_2 decreases rapidly when r_{p1} is chosen higher. From the data listed for the total characteristic velocity, $\Delta V_1 + \Delta V_2$, velocity is reduced more than 100 m/s for the case of $r_{p1} = 6430$ km. This is a 57.8% fuel saving over the Hohmann transfer. For the realistic optimal AOT, the fuel saving is about 59.6%. It has been pointed out that the minimum ΔV_2 is achieved when the exit flight-path angle $\gamma_e = 0$. However, the targeting error increases due to a smaller γ_e. Such an increase is because, for this type of trajectory, all forces involved have the same order

of magnitude, thus invalidating the basic foundation of the MAE method.

Conclusions

This work has presented an explicit guidance of AOT using the analytical solutions derived by the method of MAE. AOT comprises three consecutive phases: a descending phase, an atmospheric fly-through at the lower layers of atmosphere with constant altitude guidance, and an ascending flight targeting the desired apogee. Explicit control laws for trajectory tracking and constant altitude guidance via lift modulation are obtained in terms of the current states of the vehicle. A feedback linearization technique is also applied to generate pseudocontrols for compensating the nonlinear terms in the motion of the vehicle, thereby ensuring the stability of the trajectory. Feedback control is then used to guide the vehicle along the nominal trajectory, whereas a matched asymptotic solution targeting the required apogee is available for trajectory tracking as well as determining the pull-up condition. Because the reference trajectory data are produced analytically, the requirement is decreased for computer resources in terms of power and storage space. The guidance algorithms are tested under the targeting dispersions of atmospheric variations. Simulation results of this explicit guidance by utilizing the matched asymptotic solution indicate that the control algorithms can effectively control both the trajectories in the lower atmosphere and in the exit phase. Although many optimal, suboptimal, or near-optimal trajectories have been developed, whether these controls can be feasibly implemented remains an open question. The approach proposed herein and its analytical formulas should be useful for mission planning and onboard guidance.

Acknowledgment

The authors would like to thank the National Science Council of the Republic of China for financially supporting this research under Contract NSC-87-2612-E-014-002.

References

[1]Walberg, G. D., "A Survey of Aeroassisted Orbit Transfer," *Journal of Spacecraft and Rockets*, Vol. 22, No. 1, 1985, pp. 3–18.

[2]Mease, K. D., "Optimization of Aeroassisted Orbital Transfer: Current Status," *Journal of Astronautical Sciences*, Vol. 36, Nos. 1/2, 1988, pp. 7–33.

[3]Vinh, N. X., Johannesen, J. R., Mease, K. D., and Hanson, J. M., "Explicit Guidance of Drag-Modulated Aeroassisted Transfer Between Elliptical Orbits," *Journal of Guidance, Control, and Dynamics*, Vol. 9, No. 3, 1986, pp. 274–280.

[4]Lee, B., and Grantham, W. J., "Aeroassisted Orbital Maneuvering Using Lyapunov Optimal Feedback Control," *Journal of Guidance, Control, and Dynamics*, Vol. 12, No. 2, 1989, pp. 237–242.

[5]Miele, A., and Wang, T., "Near-Optimal Highly Robust Guidance for Aeroassisted Orbital Transfer," *Journal of Guidance, Control, and Dynamics*, Vol. 19, No. 3, 1996, pp. 549–556.

[6]Gamble, J. D., Cerimele, C. J., Moore, T. E., and Higgins, J., "Atmospheric Guidance Concepts for an Aeroassisted Flight Experiment," *Journal of Astronautical Sciences*, Vol. 36, Nos. 1/2, 1988, pp. 45–71.

[7]Naidu, D. S., *Aeroassisted Orbital Transfer: Guidance and Control Strategies*, Lecture Notes in Control and Information Sciences, Vol. 188, Springer-Verlag, London, 1994, pp. 1–30.

[8]Vinh, N. X., and Kuo, Z.-S., "Improved Matched Asymptotic Solutions for Deceleration Control During Atmospheric Entry," *Acta Astronautica*, Vol. 40, No. 1, 1997, pp. 1–11.

[9]Kuo, Z.-S., and Vinh, N. X., "Improved Matched Asymptotic Solutions for Three-Dimensional Atmospheric Skip Trajectories," *Journal of Spacecraft and Rockets*, Vol. 34, No. 4, 1997, pp. 496–502.

[10]Nayfeh, A. H., *Perturbation Methods*, Wiley, New York, 1973, pp. 110–125.

[11]Kevorkian, J., and Cole, J. D., *Perturbation Methods in Applied Mathematics*, Springer-Verlag, New York, 1981, pp. 20–29.

[12]Lagerstrom, P. A., *Matched Asymptotic Expansions*, Springer-Verlag, New York, 1988.

[13]Ardema, M. D., "Solution of the Minimum Time-to-Climb by Matched Asymptotic Expansions," *AIAA Journal*, Vol. 14, No. 7, 1976, pp. 843–850.

[14]Chobotov, V. A., Karrenberg, H. K., Chao, C. C., Miyamoto, J. Y., Lang, T. J., Kechichian, J. A., and Johnson, C. G., *Orbital Mechanics*, 2nd ed., AIAA, Reston, VA, 1996, pp. 94–109.

[15]London, H. S., "Change of Satellite Orbit Plane by Aerodynamic Maneuvering," *Journal of the Aerospace Sciences*, Vol. 29, No. 3, March 1962, pp. 323–332.

[16]Mease, K. D., and Vinh, N. X., "Minimum-Fuel Aeroassisted Coplanar Orbit Transfer Using Lift-Modulation," *Journal of Guidance, Control, and Dynamics*, Vol. 8, No. 1, 1985, pp. 134–141.

[17]Chapman, D. R., "An Approximate Analytical Method for Studying Entry into Planetary Atmospheres," NASA TR R-II, 1959.

[18]Loh, W. H. T., "A Second-Order Theory of Entry Mechanics into a Planetary Atmosphere," *Journal of the Aerospace Sciences*, Vol. 29, No. 10, 1962, pp. 1210–1221.

[19]Yaroshevskii, V. A., "The Approximate Calculation of Trajectories of Entry into the Atmosphere," P. 1 and 2, *Kosmicheskie Issledovaniya*, No. 2, Vol. 4-5, 1964 (translation).

[20]"U.S. Standard Atmosphere, 1976," National Oceanic and Atmospheric Administration, Rept. NOAA-S/T 76-1562, U.S. Government Printing Office, Washington, DC, 1976.